J. Astrophys. Astr. (1983) **4**, 271–288

Modelling of Seeing Effects in Extragalactic Astronomy and Cosmology

S. Djorgovski *Department of Astronomy, University of California, Berkeley, CA 94720, USA*

Received 1983 September 1; accepted 1983 December 7

Abstract. Convolution methods for modelling of astronomical seeing effects have been investigated. The advantages and disadvantages of several techniques are discussed, and particular attention is given to the fast Fourier transform (FFT) method. This method is then applied to two classes of problems, the structure of cores of elliptical galaxies, appearance of distant galaxies and the consequences of seeing effects in some cosmological tests. Estimates are presented for dimming of the central surface brightness and changes in the apparent core radius for elliptical galaxies, as well as seeing-induced changes in ellipticity. Modelling of galaxies with stellar nuclei has also been performed. Some consequences of these effects in investigations of dynamics of elliptical galaxies are addressed briefly. The influence of seeing in observational cosmology is discussed in the context of Hubble diagram (m–z) tests. It is shown that inadequate compensation for seeing effects can seriously distort the conclusions in such tests. Some suggestions for future work in this direction are offered.

Key words: galaxies: elliptical—cosmology—Earth's atmosphere: seeing

1. Introduction

Optical astronomy suffers a severe case of blurred vision. The light which comes—almost undisturbed—from distant objects encounters at the end of its journey the Earth's atmosphere, a telescope, and a detector. There it suffers a variety of refraction and scattering processes, which dismally distort the images it carries. Mathematically, the smearing process can be represented as a two-dimensional convolution of the true light profile (as projected on the sky), and the point-spread function (hereafter PSF) of the atmosphere + telescope + detector system. Astronomy is now at the stage where this information barrier is one of the most serious. Certainly, space-based observations will help us resolve many of the mysteries on scales smaller than an arcsec; but most of optical astronomy will still be done from the ground for many decades to come. Thus we must try our best to recover some of that hidden information, or, at least, understand quantitatively the effects of seeing.

The main purpose of this paper is to demonstrate how application of the simple fast Fourier transform (FFT) techniques can be used to model the seeing effects, and thus, hopefully, helps us regain some of the hidden morphological information. The methods discussed here can also be applied in planning of space-based observations.

The light distributions in cores of elliptical galaxies and bulges of disk systems have been a subject of lively debate and controversy. How is the true light distribution changed due to seeing, and what can we say about it by using presently available ground-based observations? The problem was approached by several authors in the past, *e.g.*, Frandsen & Thomsen (1979, 1980), Nieto (1980, 1983a, b), Bendinelli, Parmeggiani & Zavatti (1981), Schweizer (1979, 1981), Lauer (1983), Djorgovski (1981), and Capaccioli & de Vaucouleurs (1983). It is of interest to consider both radial and azimuthal redistribution of light.

Most authors have neglected the effects of seeing in optical observational cosmology, although some have tried to account for them by assuming a Gaussian PSF. A more realistic approach is needed, as shown in Section 6. Seeing effects may systematically bias the cosmological tests which rely on the shape of the light profiles of faint galaxies, and also the interpretations of active galactic nuclei (AGN) and quasi-stellar objects (QSO).

2. Numerical technique employed

Fourier transforms are a well-known tool in the image-processing community for modelling of this kind of problems but are still underutilized by the optical astronomers. In this work, the two-dimensional FFT technique was applied, which made it possible to survey a larger portion of parameter space than was investigated by others, and address some new problems. Descriptions of the profiles and PSFs used are given in Section 3.

The real-even symmetry property of all model functions was used (of which elliptical symmetry is a special case). Namely, the Fourier transform of a real-even function is real-even itself, so that only a half of each row or column needs to be transformed, and therefore only a quarter of the total array needs to be considered. The basic algorithm was developed by Connes (1971). In the present work, arrays of size 129^2 (128 + central row and column), corresponding to a full image size of 256 by 256 elements, 257^2 and 513^2 were used. Arrays of 65^2 do not provide sufficient dynamical range in terms of widths of profiles and transforms. The pixel size chosen for the profile domain was 0.1 arcsec, with the exception of investigations of effects relevant in cosmology (Section 6), where the scale was optimized from case to case, so as to minimize the computational errors.

One important part of the Fourier procedure is edge tapering (windowing, or apodizing). In the one-dimensional case it is accomplished easily, usually by using a cosine taper. However, in the two-dimensional case unsuspected difficulties arise. Most tapers commonly used in the one-dimensional case, such as cosine or Gaussian tapers, when cylindrically extended and applied to a two-dimensional case, produce spurious wave patterns in the Fourier domain. After some experimentation, it was concluded that the optimal taper consists of the (profile-domain) convolution of two cylinders, here mostly with radii 11.5 arcsec and 1 arcsec. This function is represented by a flat-topped cylinder which extends up to a radius of 10.5 arcsec, with a smooth transition to

zero, which ends at a radius of 12.5 arcsec. Different radii were used in the cosmological investigations (Section 6), optimized for a given redshift. A similar, but narrower taper was used in the frequency domain, typically flat up to the 50th component for the case of 129^2 transforms (where numerical noise became serious), and with the same smooth transition to zero onwards. Although it is desirable to keep as much of the high-frequency information as possible, in order to preserve the sharpness of the central peak, most of the noise power is also at high frequencies.

Another problem is that sampling along the array diagonal is inferior to sampling in the first (central with respect to the image) row or column, because a $\sqrt{2}$ times larger distance has to be sampled with the same number of pixels. This induces the loss of circular (or elliptic) symmetry in the transform domain (the structure of transforms resemble four- or eight-rayed stars), and, for some drastic cases, in the profile domain as well. There does not seem to be any way around this difficulty, except to apply as large an array as possible, and thus improve the sampling altogether. Experiments have shown that for the dynamical range used here a 129^2 quadrant is relatively free from this problem (and certainly it is safe in the core region, which is of interest here), whereas the 65^2 case suffers from it appreciably; for the higher dimension arrays, the effect becomes negligible.

A part of this effect is undoubtedly due to the 'wrap-around' of convolution, which is a form of aliasing (see Bracewell 1965). If the sum of the radii to which the two components extend is larger than the size of the array used for convolution, as was often the case in this investigation, there will be some wrap-around leakage. The cure is to taper the two in such a way that the sum of outer taper radii is less than the array size This, however, may require an inadmissibly large array. If the cores of convolutions are of primary interest, and/or the profiles' tails are not too fat, this effect may be comfortably ignored; if not, one has to be very careful in interpreting the results at large radii.

The present programs were tested by doing a large number of convolutions with functions where the analytical result is known (*e.g.* Gaussians among themselves, or modified Hubble profiles among themselves). The relative errors are negligible in the centre, and increase up to about 0.005–0.05 at $r_{conv} = 10$ arcsec. The errors are highest when high contrast in characteristic size is present (*e.g.*, galaxy with $r_c = 0.02$ arcsec and GE.5 PSF). At large radii, the 'wrap-around' phenomenon contributes to the errors. The errors were substantially smaller when larger-size arrays were used (257^2 or 513^2).

Other numerical methods for performing convolutions were also investigated, and it is of interest to compare them. The most straightforward technique is the numerical evaluation of the integral

$$I^{app}(x, y) = \int\int_{-\infty}^{\infty} I^{true}(u, v)\, S(x-u, y-v)\, du\, dv, \tag{1}$$

where S denotes the PSF. This technique has a drawback of being computationally slow, and thus expensive.

An alternate method for performing two-dimensional convolutions is based on the Fourier projection theorem (Budinger & Gulberg 1974). In general, the two-dimensional Fourier transform of a function $f(x, y)$ is given by

$$F(u, v) = \int\int_{-\infty}^{\infty} f(x, y) \exp[-2\pi i (xu + yv)]\, dx. \tag{2}$$

The central row of the transform (*i.e.*, where frequencies $v = 0$) is then given by

$$F(u,0) = \int\int_{-\infty}^{\infty} f(x,y) \exp[-2\pi i u x] \, dx dy, \tag{3a}$$

or

$$F(u) = \int_{-\infty}^{\infty} m(x) \exp[-2\pi i u x] \, dx, \tag{3b}$$

where

$$m(x) = \int_{-\infty}^{\infty} f(x,y) \, dy \tag{4}$$

are marginals (projections) of the function $f(x,y)$ in the y-direction. Thus, the central row of the two-dimensional Fourier transform can be computed as *one-dimensional* transform of marginals summed perpendicularly to the corresponding axis. This will hold for an arbitrary position angle. If the function $f(x,y)$ is circularly symmetric, so is its transform; computing the central row is then equivalent to computation of the whole (two-dimensional) transform due to this symmetry property. If this is the case, marginals can be evaluated from

$$m(x) = 2 \int_0^{\infty} \frac{f(r) r \, dr}{x \sqrt{r^2 + x^2}}. \tag{5}$$

Unlike the 2-dimensional FFT, this method does not require large computing storage, and is computationally about three times faster for performing convolutions. However, it yields 2–10 times the computational errors of the FFT, within about two convolution core radii, and rapidly increasing errors beyond that. This is presumably due to the (inevitable) discretization of radial profiles. It may be profitable in some situations to use this method with very-large-dimension arrays, thus improving on both sampling and dynamical range. However, computing time increases dramatically with array dimension, and the gain in accuracy increases slowly.

In a case of circular symmetry, a 1-dimensional Hankel transform (Bracewell 1965), is equivalent to the full 2-dimensional Fourier transform. For *some* functional forms, it has simple analytical formulation, and it may be evaluated faster than the FFT, but in general this need not be the case. Numerical techniques for evaluating Hankel transforms are discussed in Siegman (1977) and Oppenheim, Frisk & Martinez (1978).

Numerical evaluation of the integral (1) has errors nearly as small as the FFT, but it is computationally several times slower, even when optimal (Gaussian) quadrature techniques are employed. However, if both galaxy profile and PSF can be represented analytically (*e.g.*, de Vaucouleurs profile and a Gaussian), *and* there is circular symmetry, the direct integration method can be substantially faster. An analytical example is given by Bailey & Sparks (1983).

To summarize, if we are dealing with a profile and a PSF which can be represented analytically (note that this is *not* the case with King models and King PSF), numerical evaluation of the integral (Equation 1) is about equally good as the FFT technique; if the profile and PSF are not analytically known, but do have circular (or some other 'easy') symmetry, Fourier projection provides the quickest answer with minimal computer memory demands (unless extremely large-size arrays are used, but then it is

very slow), but it is unreliable beyond about two core radii; and finally, in a general case and/or if higher accuracy is desired, the FFT method seems to be the best choice. If both the galaxy profile and PSF possess orthobiplanar (mirror-like) symmetry, the real-even FFT algorithm should be used. The use of Hankel transforms requires further study.

More detailed discussions of the fundamental properties of Fourier transforms are given in Bracewell (1965). A classical astronomically-oriented introduction is given by Brault & White (1971).

3. Profiles and PSFs used

Seven different PSFs were used, six different circular galaxy models and one elliptical galaxy model (E5, King model with $c = 2.25$), with ten core radii each, and several 'disk galaxy' profiles, intended for morphological comparisons. Altogether, several hundred convolutions were performed.

The PSFs used are listed in Table 1. Functions GE2, GE1 and GE.5 are defined as a Gaussian core plus exponential wings attached to it at 2σ. The wings have slopes of 2, 1 and 0.5 mag per arcsec respectively. Function GES1 is a 'worsened case' of GE1: it has wings attached at 1σ. If a Gaussian had 2 mag exponential wings attached at 1σ it would be for all practical purposes identical to GE2, and it was therefore omitted. The function King (1971) is given in that reference, and it is the best available empirically determined PSF. Function Moffat (1969) is the analytical approximation suggested in that reference, and based on a study of photographic stellar images

$$S(r) = [1 + (r/1.465)^2]^{-2.72} \tag{6}$$

where r is in arcsec. The semiempirical PSF suggested by Valdes, Jarvis & Tyson (1981) has been found very similar to King (1971) or Moffat (1969) PSFs in the core, if properly scaled; we assume that it would show similar effects to those two. The same should hold for the PSF shown in Capaccioli & de Vaucouleurs (1983).

Table 1. The point-spread functions used.

Designation	Description	Energy in wings
G or Gaussian	Gaussian with $\sigma = 0.75$ arcsec	0.500
GE2	Gaussian core with $\sigma = 0.75$ arcsec and exponential wings with slope of 2 mag arcsec^{-1} attached at 2σ	0.632
GE1	As above, but slope of wings 1 mag arcsec^{-1}	0.794
GE.5	As above, but slope of wings 0.5 mag arcsec^{-1}	0.914
GES1	Wing slope 1 mag arcsec^{-1}, attached at 1σ	0.776
King (1971)	Empirical PSF determined by King	0.616
Moffat (1969)	Semiempirical PSF suggested by Moffat	0.645

Note:
The energy in wings is the fraction of the total energy in a stellar image contained *beyond* the half-maximum isophote. The numbers given have been evaluated analytically for all but the King PSF, where numerical integration was used on the tapered function, as employed in this work. The original King (1971) PSF has divergent wings.

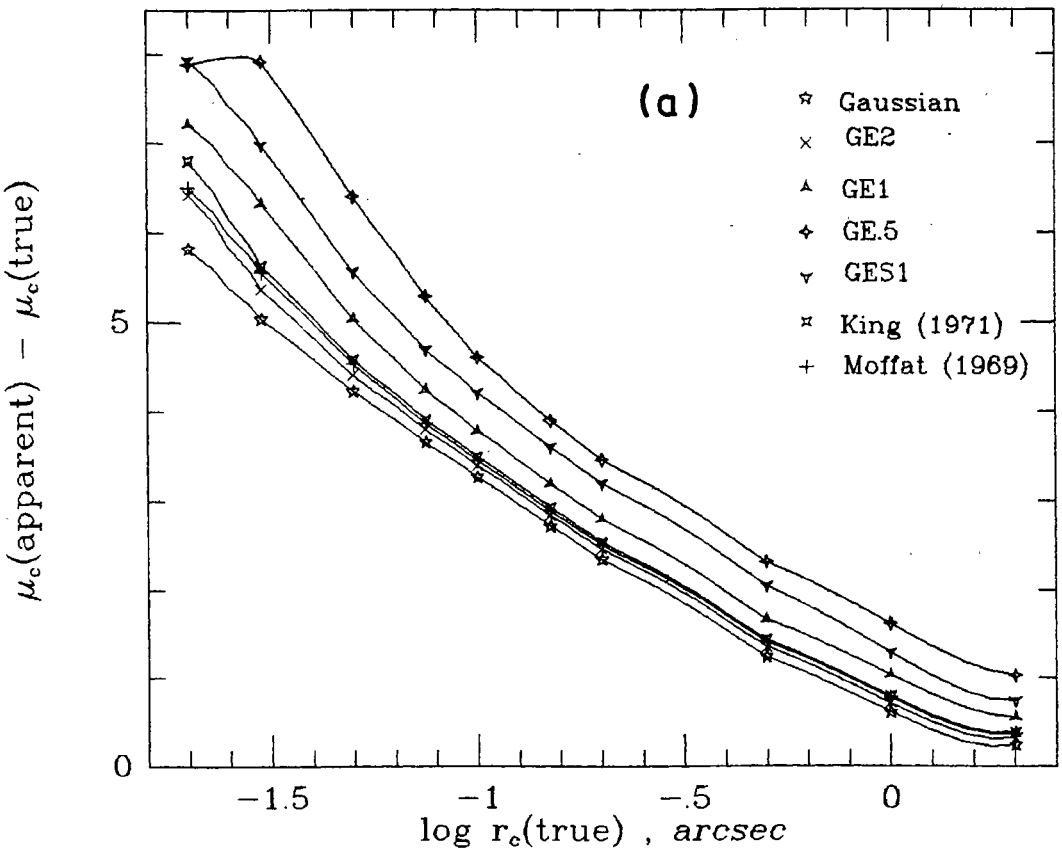

Figure 1. (a) Dimming of central surface brightness and (b) apparent core radius (defined as half-width at half maximum) as a function of true core radius for King-model galaxy with $c = 2.5$. Different symbols represent different PSFs. Lines connecting the points were produced by cubic Lagrangian interpolation.

A pure Gaussian certainly underestimates the seeing; a realistic PSF should have some wings, of exponential or power-law nature. The PSFs for different telescopes, detectors and atmospheric conditions will never have any universal form, and this fact alone eliminates any single-parameter PSF. Power laws have their justification in theories of atmospheric turbulence (Black 1980; Woolf 1982; Reiger 1963). Let us note here that functions GE.5 and GES1 almost certainly overestimate the importance of the wings, and constitute a kind of upper limit, as contrasted to a Gaussian. Thus, it appears that the range of possible seeing has been covered fairly well with the present set of PSFs. The functions King (1971), GE2 and Moffat (1969) give very similar results.

An important question is, how much of the total energy is removed to the wings of a PSF? Function King (1971) has outer wings with the slope of -2; for Schmidt plates, Su & Simkin (1983) find that the slope of wings is -1.9 as far as they could measure it (10 arcmin or more); Kormendy (1973) finds power-law wings with the slope of -1.54. Those divergent forms must taper off at some radius, but it is possible that in some cases unsuspectedly large fraction of the total energy is hidden in the wings of a PSF.

Excellent reviews of the general topic of astronomical seeing are given by Woolf (1982) and Young (1974). Seeing as a physical phenomenon seems to be now well understood. For analysis of 'real' data, it may be more profitable to consider the effects

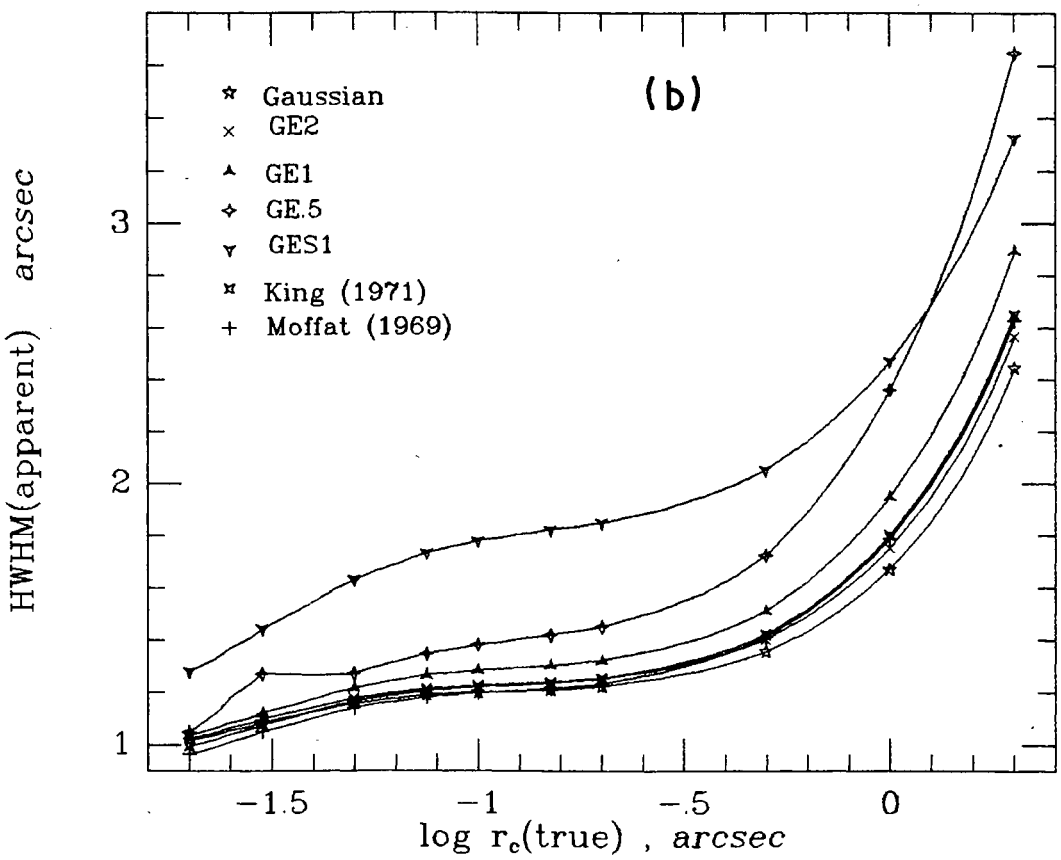

of seeing convolutions in the Fourier domain; functional forms for the PSFs given by Woolf (1982) may be used for such a purpose. We opt here to present all results in the profile domain, for the sake of intuitive clarity.

4. Structure of the cores of elliptical galaxies

Galaxy models used include three King (1966) single-mass, nonrotating models with concentration indices $c = 2.25$, 2.5 and 2.75. These models are not represented by any simple analytical formula, but are evaluated numerically, following the precepts of the King paper. For this purpose a computer program developed by Ivan King and John Retterer was used. Also used was the well-known de Vaucouleurs profile

$$I(r) = I(0)\exp[-7.66925\,(r/r_e)^{1/4}], \tag{7}$$

where r_e is the equivalent (half-the-total-light) radius; modified Hubble profiles

$$I(r) = I(0)\,[1 + (r/r_c)^2]^{-1}, \tag{8}$$

where r_c is the core radius, and a further modification

$$I(r) = I(0)\,[1 + (r/r_c)^2]^{-0.8}, \tag{9}$$

which should represent fairly well a cD galaxy. These forms compare well with some published observed profiles (King 1978; Oemler 1976). The set of core radii used were 0.02, 0.03, 0.05, 0.075, 0.1, 0.15, 0.2, 0.5, 1 and 2 arcsec for all profiles but de

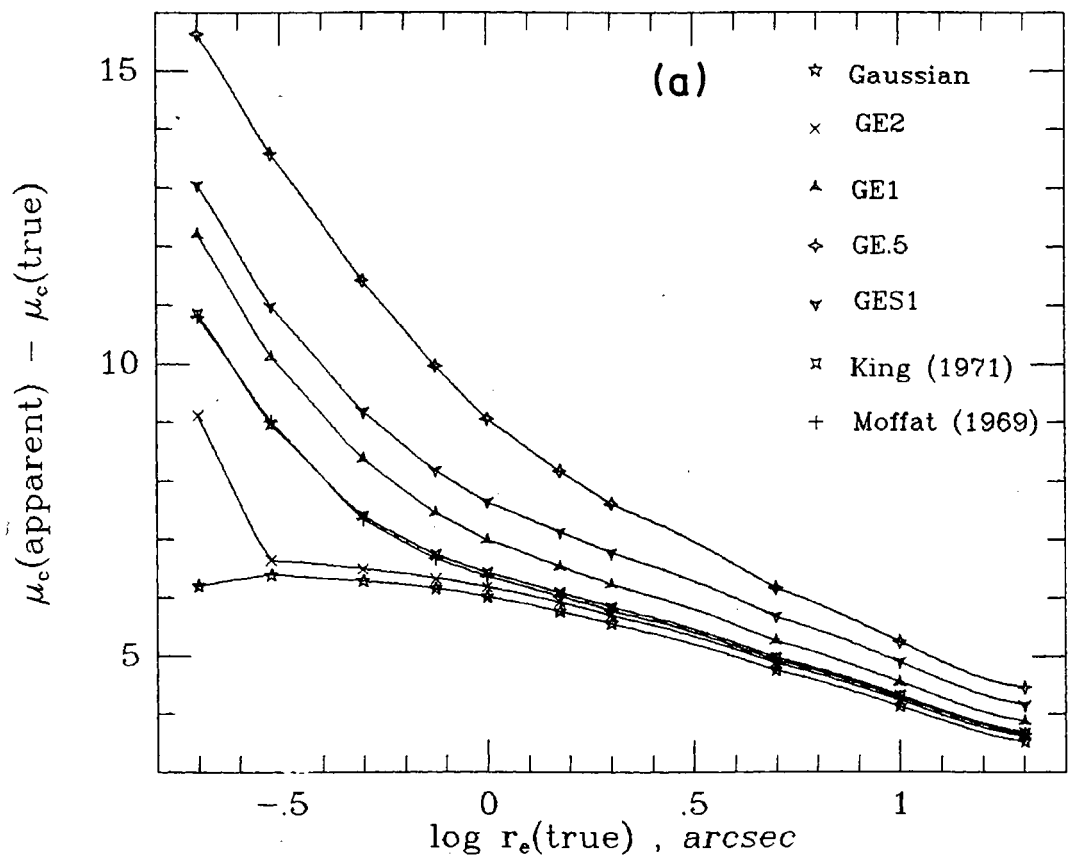

Figure 2. (a) Dimming of central surface brightness and (b) apparent core radius (defined as half-width at half maximum) for de Vaucouleurs profile.

Vaucouleurs', where r_e values which were ten times higher were chosen, in order to produce good correspondence in the shapes of the profiles. A small subset of these has been investigated already by Schweizer (1981), and our results are in excellent mutual agreement.

The two most natural physical quantities which represent the influence of seeing in the cores are the apparent core radius (here operationally defined as a half-width at half maximum, hereafter HWHM) and the central-surface-brightness dimming. Figs 1 and 2 demonstrate the change of those quantities for two of the six galaxy models employed, as functions of true core radius (or equivalent radius for the case of de Vaucouleurs profiles). The results for other models do not differ qualitatively from those shown. These figures should serve as an estimator of seeing effects. One can also make some conclusions about the influence of seeing upon mass-to-light ratios as derived from the King-Minkowski formula (see, *e.g.* Schechter 1980):

$$M/L \sim \sigma_v^2/(I_0 r_c) \tag{10}$$

The apparent ratios get larger as seeing gets more important, and the corrections may be as large as a factor of 5, for the change of $I_0 r_c$ alone. Also, the measurements of the nuclear or near-nuclear velocity dispersions and of rotational velocities pertain to a mixture of light coming from different radii. An example of this phenomenon is provided in modelling of the bulge velocity dispersions in M31 by Ruiz (1976) and

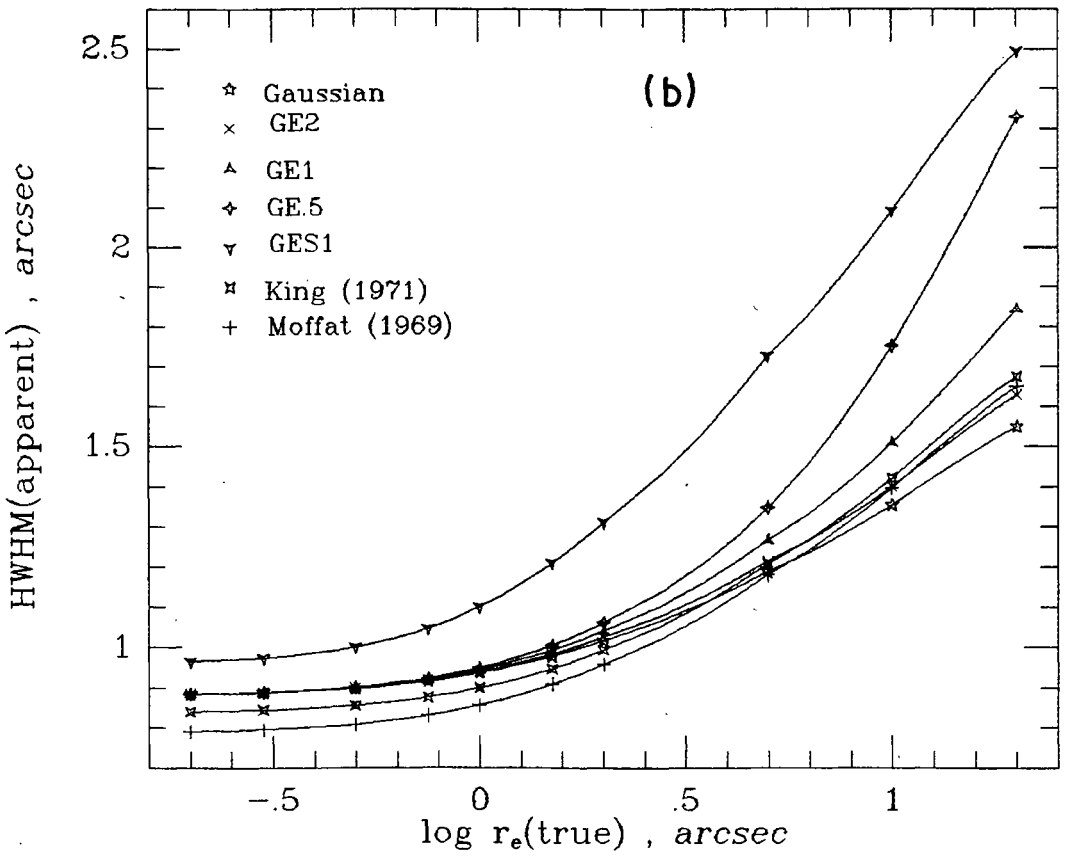

Whitmore (1980). They conclude that the corrections to observed velocity dispersion (due to seeing) may reach $\sim$ 20 per cent, even in this relatively well-resolved case. Peterson & Collins (1983) present work in a similar direction, in their investigation of Seyfert nuclei.

The influence of seeing on apparent ellipticities in galactic cores has also been investigated. A galaxy given by the King $c = 2.25$ model and E5 shape throughout was convolved with all seven PSFs, for all ten values of r_c (major axis). Plots of the central dimming and the apparent core radius *vs.* the true core radius are analogous to those shown on Figs 1 and 2. Fig. 3 shows runs of ellipticity for the apparent core radius isophote. Notice that even in the cases which would otherwise be termed as 'seeing resolved', apparent ellipticity still does not reach the true value of 0.5. Possible isophotal twists and ellipticity changes near the centre will also pass undetected. An example of such ellipticity round-off in M87 can be found in de Vaucouleurs and Nieto (1979). The present results are in agreement with the earlier, pioneering study by Capaccioli & Rampazzo (1980).

Fig. 4 shows runs of ellipticity *vs.* radius for a particular value of $r_c = 0.1$ aresec. 'Bumps' (ellipticity inversions) which appear for the cases of wide PSFs occur on all such plots, and their prominence is dependent on the degree to which seeing dominates the profile. A part of the effect may be caused by the artificial rounding of the outer isophotes due to tapering. This illustrates one of the inherent dangers of convolution: it is a non-local process, and one has to worry about the whole picture.

One of the main motivations for this study was to try to find a set of observationally

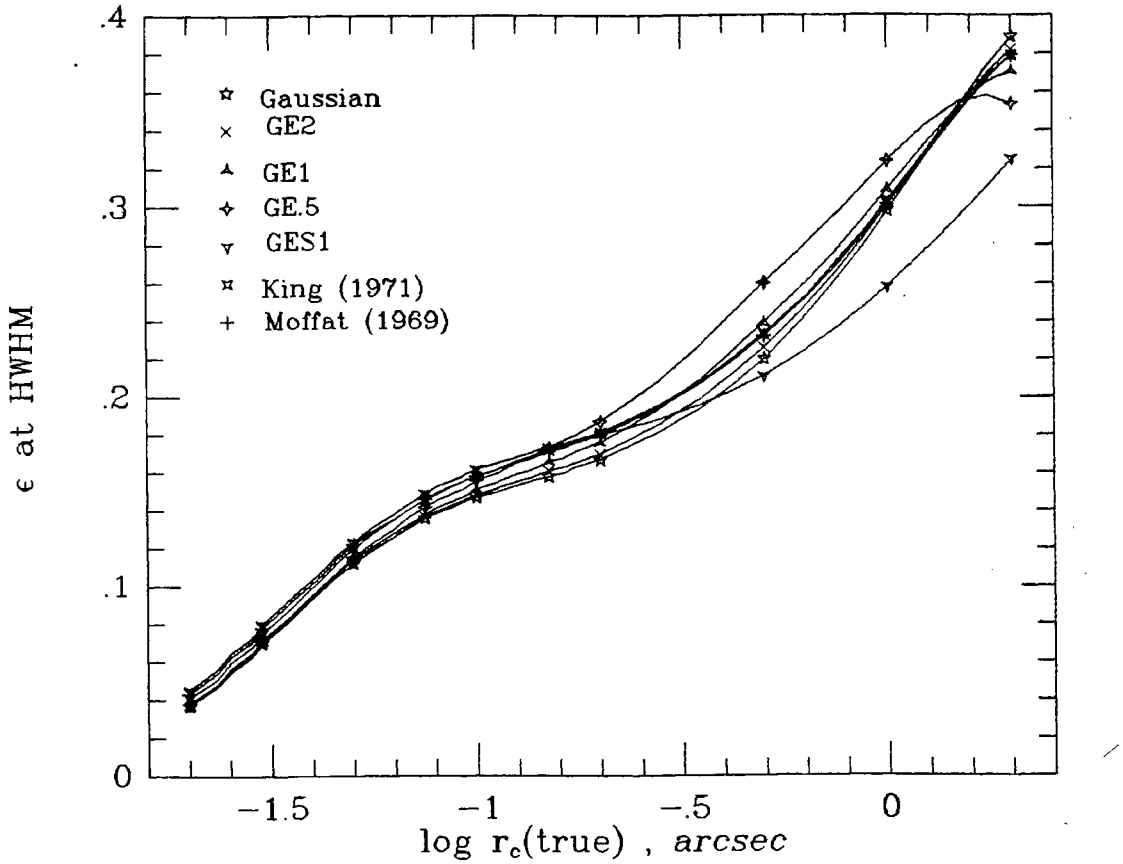

Figure 3. Ellipticity of the half-maximum isophote as a function of true core radius (major axis), for E5 King model with $c = 2.25$. Different symbols correspond to different PSFs.

definable quantities which would allow us to estimate the shape and the radial scale of the original profile. I have tried numerous correlations of surface brightness and magnitudes at different radii, in various combinations, but without much success. The seeing convolution makes intrinsically different profiles similar in their observable properties, and the subtle differences that do remain will certainly be lost in any noise that is present in the real data. However, if one is willing to assume *a priori* the shape of the original profile, it is possible to estimate the changes in intensity and radial scales, if the radial scale for the PSF is known. Trends such as those shown in Figs 1 and 2 can be used for that purpose. This becomes increasingly more difficult as the galaxy is more seeing-dominated (the curves steepen), but some estimate can be made.

For real data, some image deconvolution method (such as Wiener filtering or Maximum Entropy) can improve the resolution only by a factor of 2 or 3 (depending on S/N and sampling), but hardly much beyond that. There are some substantial problems, related to the high-frequency noise, non-isoplanicity (spatial variability across the field) of the PSF, and sampling. Lauer (1983) gives some discussion of these difficulties. A very sobering account of limits to seeing deconvolutions is given by Young (1974). For investigations of large samples some insight may be gained by comparing observed profiles with convolution families such as those shown here, and this may be a better way of approach. Suggestions in this spirit were also made by de Vaucouleurs (1979).

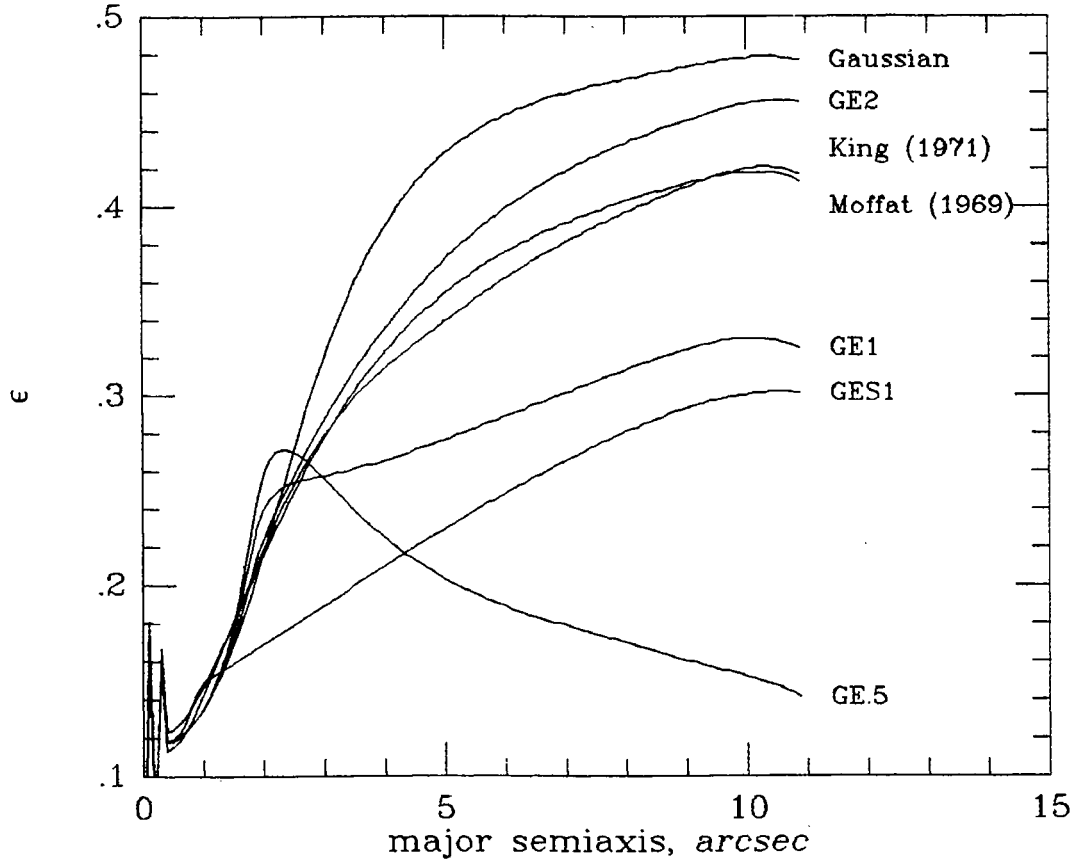

Figure 4. Ellipticity at a given semimajor axis for E5 galaxy (King, $c = 2.25$) with $r_c = 0.1$ arcsec. Curves are labelled with applicable PSFs. Noise at $r \leqslant 0.4$ arcsec is due to the small number of pixels enclosed.

5. Effects of stellar nuclei

Stellar nuclei (that is, PSF-shaped profiles) were added to a number of convolved galaxy profiles. Relative contributions of stellar core to the total light were 10, 50 or 90 per cent. Also, a set of King ($c = 2.5$) profiles was convolved with the King (1971) PSF, using finer sampling, and added to stellar cores whose contribution to the total light spanned ten values, from 1 to 90 per cent. Applications of this study may include detectability of unresolved spikes in galactic cores, such as M32. An intriguing set of data on dwarf ellipticals by Caldwell (1983) suggests that such nuclei may be very common. Another aspect is the nature of galaxies underlying QSOs, or AGN in general.

In a seeing-dominated profile, a possible stellar nucleus can be smeared out. Our experiments show that the efficiency of seeing in hiding these nuclei depends sensitively on the ratio of characteristic scales for both galaxy and PSF (that is, r_c^{true} and HWHM), the relative contribution of the nucleus to the total light, and the form of the PSF (in particular, fraction of the total energy in the wings). As a quantitative estimator, one can use the trend depicted in Fig. 5. Even in the cases where the stellar nucleus does not produce an artifact (a central cusp) in the observed light profile, it typically *does* change its form perceptibly. Estimates of the ratio of the nuclear-to-total light in AGN systems

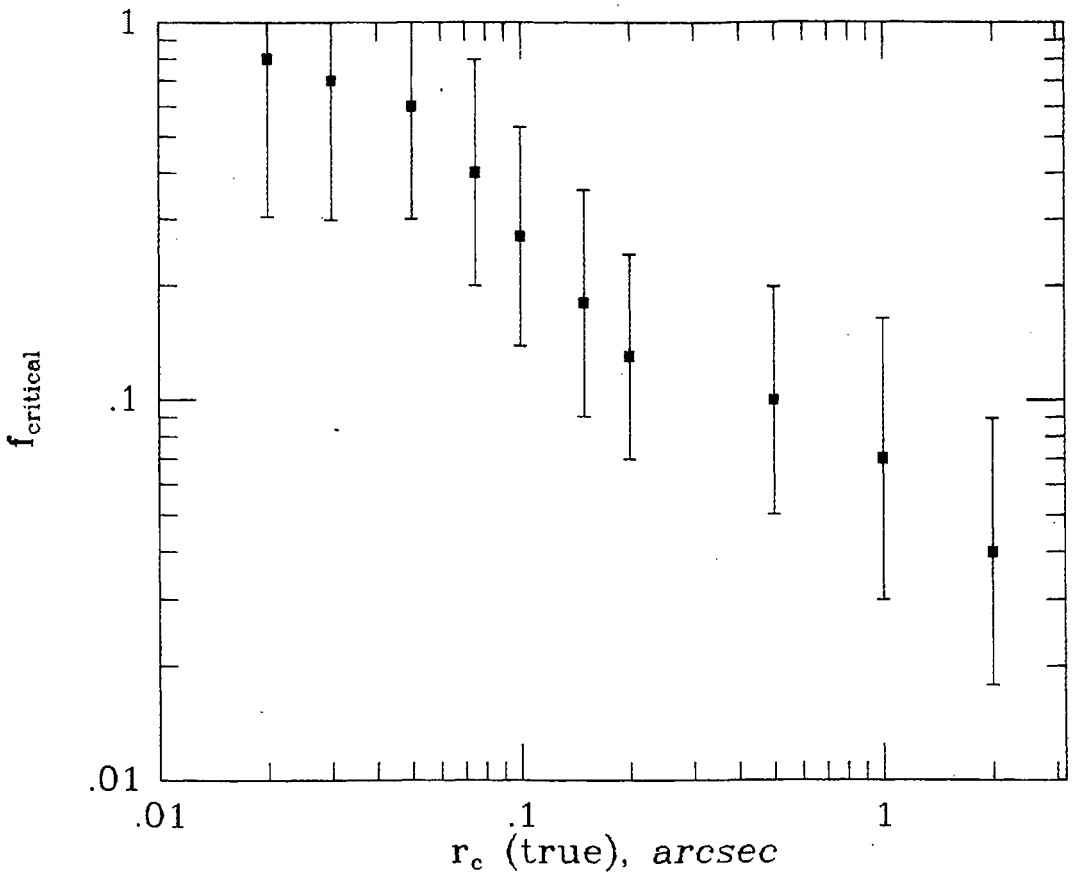

Figure 5. $f_{critical}$ is the estimated minimal relative contribution of a stellar nucleus to the total light, at which it is impossible to detect its presence from the shape of the resultant galaxy profile by inspection. Smaller contributions will pass undetected. The error bars reflect the range in which it first becomes possible to estimate that the stellar nucleus is present.

may be in appreciable error, if seeing is not taken carefully into account. An example of such a situation may be provided by Sandage's (1973) efforts in classifying and understanding N-galaxies.

In the case of galaxies underlying QSOs, the PSFs for the nucleus, galaxy and field stars may be slightly different, because the PSF will be in general mildly colour-dependent, and non-isoplanatic. This makes the usual star subtraction procedure even more prone to distort the underlying galaxy profile. The same applies to the *shape* of underlying galaxy's isophotes: seeing will make them rounder, thus biasing interpretation in favour of elliptical galaxies (*cf.* Wyckoff *et al.* 1983; Hutchings 1983).

In the same way, possible multiple nuclei (*e.g.*, due to galactic cannibalism) can be effectively hidden. Hoessel (1980) finds them in 28 per cent of the cases he was investigating, and Schneider, Gunn & Hoessel (1983) find them in 45 per cent of their clusters. A statistical estimate of how many more there can be may be obtained by setting up a grid of binuclear galaxy models (the parameters being mutual separation and intensity contrast), and convolving them with a realistic PSF. This may be a basis for an interesting future study.

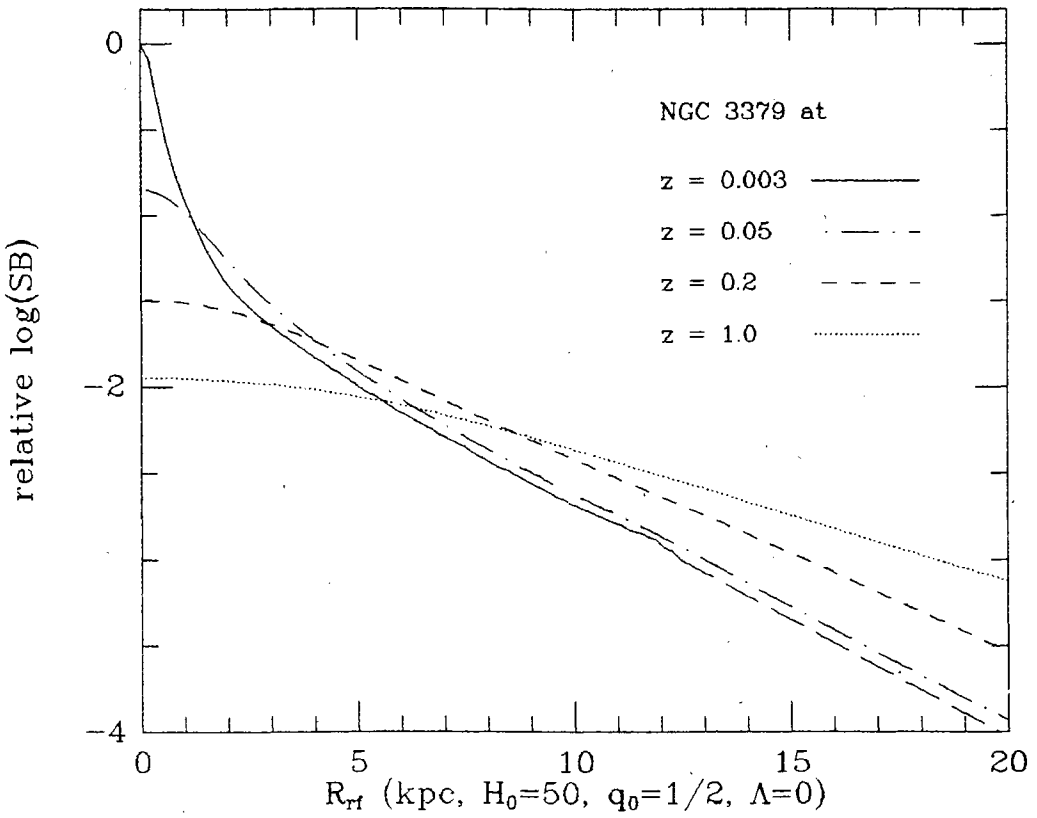

Figure 6. The profiles of NGC 3379 as observed ($z = 0.003$) and as it would appear at the higher redshifts. King (1971) PSF was used for convolutions. R_{rf} is the rest-frame radius.

6. Seeing effects in cosmology

The appearance of distant galaxies will be drastically dominated by the seeing. A simple example, shown in Fig. 6, is a good illustration. I have used surface photometry of the standard elliptical galaxy NGC 3379 (Kent & Djorgovski, in preparation), and convolved it with appropriately scaled King PSFs, in order to predict its hypothetical appearance at the higher redshifts. The central dimming shown here is due to the seeing alone, with no relativistic or evolutionary corrections. The higher-z curves climb above the lower-z ones because they are plotted on a *metric* radial scale, and a progressively larger fraction of the central light is moved outwards. Similar experiments with spiral galaxy profiles show them virtually indistinct from the elliptical ones for any $z \geqslant 0.1$, even in good seeing.

A large part of the observational cosmology done in the optical band involves distant galaxies; through their magnitudes (see, *e.g.*, Hoessel 1980; Hoessel, Gunn & Thuan 1980; Schneider, Gunn & Hoessel 1983), and their diameters (*e.g.*, Djorgovski & Spinrad 1981). It is necessary to invoke some profile-determined radial scale in order to define standard diameters for the galaxies, which would also serve as apertures for the 'standard candle' photometry. One such function is the Gunn & Oke (1975) parameter α, which is a logarithmic derivative of the total light. Hoessel, Gunn & Thuan find for their sample and assumed metric radius a mean α of 0.49 ± 0.01, which is supposed to

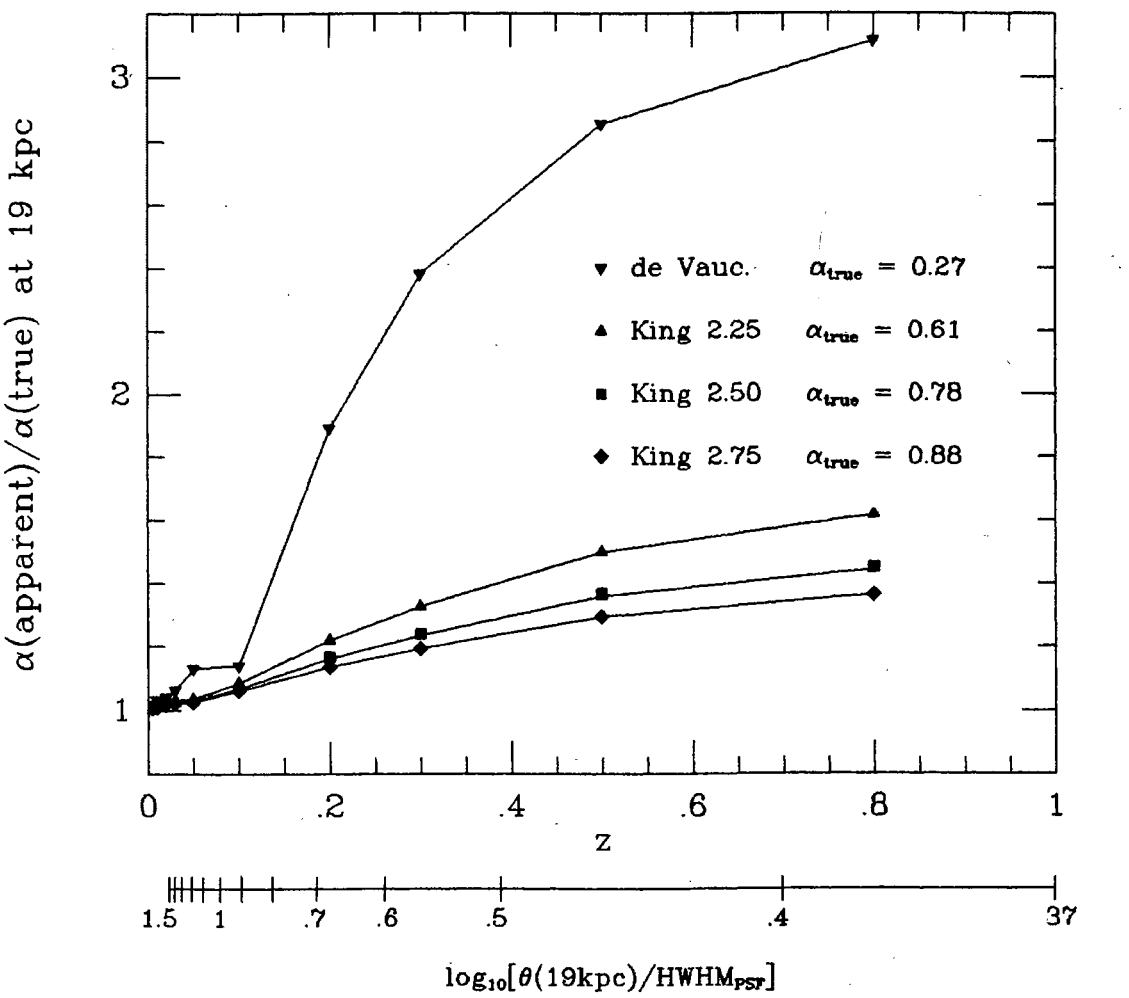

Figure 7. Ratios of the apparent and true values of the Gunn-Oke parameter alpha as a function of redshift, at the true metric radius of 19 h_{50}^{-1} kpc. The symbols represent corresponding galaxy models. For the scale below see the text.

correspond to 19 h_{50}^{-1} kpc. They have attempted to compensate for seeing effects by convolving a Hubble profile with a Gaussian. A better attempt to compensate for seeing distortion of standard apertures has been done by Schneider, Gunn & Hoessel (1983) who used a bi-Gaussian PSF and both Hubble and de Vaucouleurs profiles. Their claim is that it does not matter which galaxy model was assumed. This should be taken with some caution; their statement should be probably understood as that all convolutions look the same, but that does not guarantee the right correction to a standard aperture.

I have convolved a set of King galaxy profiles with assumed $r_c^{\rm true} = 1$ kpc ($r_e = 10$ kpc for de Vaucouleurs case) with the King (1971) PSF (HWHM = 0.95 arcsec). The galaxies were placed at distances corresponding to a set of assumed redshifts between 0.005 and 0.8, and a simple Friedmann cosmology with $H_0 = 50$ km s^{-1} Mpc^{-1} and $q_0 = \frac{1}{2}$ was assumed. The important variable is the ratio of the galaxy's metric angular diameter θ, and the PSF scale. Metric angular radii in a Friedman ($\lambda_0 = 0$) cosmology are given by the formulae (see, *e.g.*, Sandage 1972):

$$\theta(\text{arcsec}) = 0.034377\, h_{50}\, (r_{\rm gal}/\text{kpc})\, Q \qquad (12a)$$

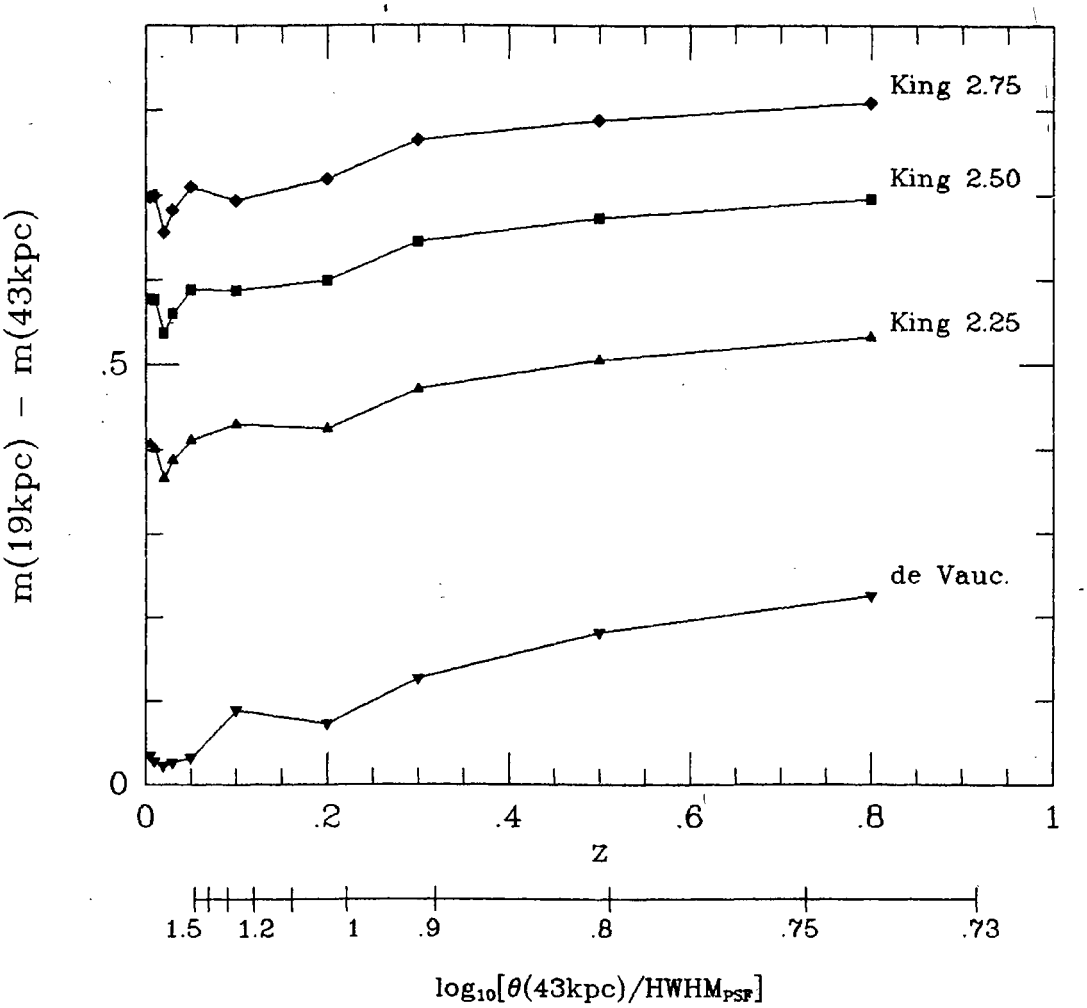

Figure 8. Magnitude difference between two metric apertures, 19 h_{50}^{-1} kpc and 43 h_{50}^{-1} kpc as a function of redshift, for a set of different galaxy models. Friedmann cosmology with $q_0 = \frac{1}{2}$ and $\lambda = 0$ is assumed. For bottom scale see the text.

where

$$Q = \frac{(1+z)^2}{z(1+z/2)} \qquad \text{for } q_0 = 0, \tag{12b}$$

$$Q = \frac{q_0^2(1+z)^2}{q_0 z + (q_0-1)[(1+2q_0 z)^{1/2}-1]} \qquad \text{for } q_0 > 0. \tag{12c}$$

These formulae can be used to calculate galaxy/PSF scale ratios for PSF widths and cosmological parameters other than those used in this study. Angular scale ratios (galaxy/PSF) are plotted for convenience in Figs 7 and 8.

The influence of seeing distortion on the values of parameter α is shown in Fig. 7. First, there is a systematic trend with redshift, amounting to about 30 per cent in this redshift interval. Second, there is a spread of about 20 per cent between the profiles of different morphology. The de Vaucouleurs profiles suffer from seeing much more than the King models, because of their sharp central peaks.

Fig. 8 shows the magnitude difference between two apertures, 19 h_{50}^{-1} kpc, and 43 h_{50}^{-1}

kpc, as used by another group (Sandage, Kristian & Westphal 1976). This was done by assuming the above cosmology, and computing the angular apertures directly, thus ignoring any problems which may arise in trying to get 'perfect' metric apertures from the data. These are slight systematic effects with redshifts, amounting to about 0.1 mag in this range, and the spread between the different galaxy types reaches 0.7 mag. The two groups (Hoessel, Gunn & Thuan, and Sandage, Kristian & Westphal) use some of the same objects, the same K-corrections, *etc.* However, their derived values of q_0 differ by 1–1.5, depending on assumed evolutionary corrections. When the observed magnitude difference, as stated above, is plotted against redshift, there is a scatter of about 0.6 mag, and a possible systematic trend with the redshift. (I am indebted to Richard Kron for bringing this to my attention.) Thus, seeing may account for a large part of this discrepancy.

Perhaps the only safe way in which we can do ground-based observational cosmology with these classical tests is through a statistical analysis of very large samples of galaxies (see, *e.g.* a review by Kron 1980). The study by Valdes (1982) is an important step in that direction. Another good example is given in the study of Pritchet & Kline (1981), although their conclusions are somewhat weakened by unfortunate choice of the PSF (a Gaussian). Interesting attempts to produce seeing-corrected photometry have been recently published by Thomsen & Frandsen (1983), and Schneider, Gunn & Hoessel (1983).

7. Summary and conclusions

I have discussed and compared numerical techniques for modelling of seeing effects, and applied them to some problems in extragalactic astronomy and cosmology. The modelling covered a large spectrum of relevant parameters, and led to the following conclusions:

The FFT method is generally the best way to calculate the seeing effects, but in some situations other convolution methods may be more convenient. Details of application of the FFT procedure are discussed.

The wings of the PSF are a dominating factor in seeing effects; the effects of seeing are certainly underestimated by a Gaussian PSF. Empirical and semi-empirical PSFs (King (1971), Moffat (1969) and GE2) produce very similar results, thus defining a kind of 'standard seeing', suitable for further studies.

In general, the true shape of an individual light profile cannot be determined by comparing the profile and PSF with a set of known convolutions, or by any correlation of observables associated with a profile. However, an estimate *can* be made if one decides *a priori* on the family of galaxy profiles.

Quantitative estimates for the central-surface-brightness dimming and the increase in apparent core radius have been presented. Mass-to-light ratios determined from the King-Minkowski formula (10) have a systematic error which increases with distance to a galaxy (and thus can be luminosity-dependent in magnitude-limited samples). This error can be estimated from trends such as those shown in Figs 1 and 2. Measurements of the nuclear and near-nuclear rotational velocities and velocity dispersions can be substantially polluted by mixing of light from different radii. Apparent ellipticity of galaxies can be changed substantially in the core. Isophotal twists and ellipticity

changes near the centre will pass undetected. Stellar or multiple nuclei may pass undetected as such in many cases.

Finally, it appears that all seeing-uncompensated (or partly compensated) profile-dependent corrections employed in various cosmological and galaxy evolution tests are in error. In the case of m–z (Hubble diagram) tests, or diameter-redshift tests, there are possible systematic effects which can change the derived values of q_0. A part of the observed scatter in magnitudes used in these tests may reflect differences in the galaxy profiles, in addition to any scatter in the luminosity itself.

Acknowledgements

I wish to express gratitude to Ivan King for constructive criticisms and support throughout this work, and for some crucial software used here. I would also like to thank Richard Kron for stimulating discussions about cosmological tests and the relevant effects investigated in this work. I. King, V. Lindsay and, especially, F. Schweizer provided critical reading of the manuscript. The paper benefitted greatly from the constructive remarks of two anonymous referees, for whose efforts I am very thankful. This work was partly supported through a University of California graduate fellowship, and the NSF grant AST 80-20606.

References

Bailey, M. E., Sparks, W. B. 1983, *Mon. Not. R. astr. Soc.*, **204,** 53p.
Bendinelli, O., Parmeggiani, G., Zavatti, F. 1981, preprint; partly in *ESO Conference on Scientific Importance of High Angular Resolution at Infrared and Optical Wavelengths*, Eds M. H. Ulrich and K. Kjar, ESO, p. 115.
Black, D. (Ed.) 1980, *Project Orion*, NASA SP-436.
Bracewell, R. N. 1965, *The Fourier Transform and Its Applications*, McGraw-Hill, New York.
Brault, J. W., White, O. R. 1971, *Astr. Astrophys.* **13,** 169.
Budinger, T. F., Gulberg, G. T. 1974, *Lawrence Berkeley Laboratory report* LBL-2146 (TID-4500-R61), University of California, Berkeley.
Caldwell, N. 1983, *Astr. J.*, **88,** 804.
Capaccioli, M., Ramapazzo, R. 1980, *Mem. Soc. astr. Ital.*, **51,** 491.
Capaccioli, M., de Vaucouleurs, G. 1983, *Astrophys. J. Suppl.*, **52,** 465.
Connes, J. 1971, in *Aspen International Conference on Fourier Spectroscopy*, Eds G. A. Vanasse, A. T. Stair and D. J. Baker, AFCRL-71-0019 Spec. Rep. No. 114, p. 83.
de Vaucouleurs, G. 1979, in *Photometry, Kinematics and Dynamics of Galaxies*, Ed. D. Evans, University of Texas, Austin, p. 1.
de Vaucouleurs, G., Nieto, J.-L. 1979, *Astrophys. J.*, **230,** 697.
Djorgovski, S. 1981, *Bull. Am. astr. Soc.*, **13,** 796.
Djorgovski, S., Spinrad, H. 1981, *Astrophys. J.*, **251,** 417.
Frandsen, S., Thomsen, B. 1979, *Astr. Astrophys*, **72,** 111.
Frandsen, S., Thomsen, B. 1980, in *ESO Workshop on Two-Dimensional Photometry*, Eds P. Crane and K. Kjär, ESO, p. 319.
Gunn, J. E., Oke, J. B. 1975, *Astrophys. J.*, **195,** 255.
Hoessel, J. G. 1980, *Astrophys. J.*, **241,** 493.
Hoessel, J. G., Gunn, J. E., Thuan, T. X. 1980, *Astrophys. J.*, **241,** 486.
Hutchings, J. B. 1983, preprint.
King, I. 1966, *Astr. J.*, **71,** 64.
King, I. R. 1971, *Publ. astr. Soc. Pacific*, **83,** 199.
King, I. R. 1978, *Astrophys. J.*, **222,** 1.

Kormendy, J. 1973, *Astr. J.*, **78,** 255.
Kron, R. G. 1980, *Phys. Scripta*, **21,** 652.
Lauer, T. 1983, *Ph.D. thesis*, University of California, Santa Cruz.
Moffat, A. 1969, *Astr. Astrophys.*, **3,** 455.
Nieto, J.-L. 1980, in *ESO Workshop on Two Dimensional Photometry*, Eds P. Crane and K. Kjär, ESO, p. 309.
Nieto, J.-L. 1983a, *Astr. Astrophys. Suppl. Ser.*, **53,** 247.
Nieto, J.-L. 1983b, *Astr. Astrophys. Suppl. Ser.*, **53,** 383.
Oemler, A. 1976, *Astrophys. J.*, **209,** 693.
Oppenheim, A. V., Frisk, G. V., Martinez, D. R. 1978, *Proc. Inst. electr. electron. Eng.*, **66,** 264.
Peterson, B. M., Collins, G. W. 1983, *Astrophys. J.*, **270,** 71.
Pritchet, C., Kline, M. I. 1981, *Astr. J.*, **86,** 1859.
Reiger, S. 1963, *Astr. J.*, **68,** 395.
Ruiz, M. T. 1976, *Astrophys. J.*, **207,** 382.
Sandage, A. 1972, *Astrophys. J.*, **173,** 485.
Sandage, A. 1973, *Astrophys. J.*, **180,** 687.
Sandage, A., Kristian, J., Westphal, J. A. 1976, *Astrophys. J.*, **205,** 688.
Schechter, P. 1980, *Astr. J.*, **85,** 801.
Schneider, D. P., Gunn, J. E., Hoessel, J. G. 1983, *Astrophys. J.*, **268,** 476.
Schweizer, F. 1979, *Astrophys. J.*, **233,** 23.
Schweizer, F. 1981, *Astr. J.*, **86,** 662.
Siegman, A. E. 1977, *Optics Lett.*, **1,** 13.
Su, H. J., Simkin, S. M. 1983, *Bull. Am. astr. Soc.*, **14,** 884; and a preprint.
Thomsen, B., Frandsen, S. 1983, *Astr. J.*, **88,** 789.
Valdes, F., Jarvis, J., Tyson, J. 1981, *Bell Laboratories Technical Memorandum* 81-11354-8.
Valdes, F. 1982, *Bell Laboratories (Holmdel) preprint* 331–44.
Whitmore, B. C. 1980, *Astrophys. J.*, **242,** 53.
Woolf, N. J. 1982, *Rev. Astr. Astrophys.*, **20,** 367.
Wyckoff, S., Wehinger, P. A., Gehren, T., Fried, J., Spinrad, H., Tapia, S. 1983, in 24*th Liège Coll.: Quasars and Gravitational Lenses* (in press).
Young, A. T. 1974, *Astrophys. J.*, **189,** 587.